

# Neural Locus of Color Afterimages

Qasim Zaidi,<sup>1,\*</sup> Robert Ennis,<sup>1</sup> Dingcai Cao,<sup>2</sup> and Barry Lee<sup>1,3</sup>

<sup>1</sup>Graduate Center for Vision Research, State University of New York, College of Optometry, New York, NY 10036, USA

<sup>2</sup>Department of Surgery, The University of Chicago, Chicago, IL 60637, USA

<sup>3</sup>Max Planck Institute for Biophysical Chemistry, 37077 Gottingen, Germany

## Summary

After fixating on a colored pattern, observers see a similar pattern in complementary colors when the stimulus is removed [1–6]. Afterimages were important in disproving the theory that visual rays emanate from the eye, in demonstrating interocular interactions, and in revealing the independence of binocular vision from eye movements. Afterimages also prove invaluable in exploring selective attention, filling in, and consciousness. Proposed physiological mechanisms for color afterimages range from bleaching of cone photopigments to cortical adaptation [4–9], but direct neural measurements have not been reported. We introduce a time-varying method for evoking afterimages, which provides precise measurements of adaptation and a direct link between visual percepts and neural responses [10]. We then use *in vivo* electrophysiological recordings to show that all three classes of primate retinal ganglion cells exhibit subtractive adaptation to prolonged stimuli, with much slower time constants than those expected of photoreceptors. At the cessation of the stimulus, ganglion cells generate rebound responses that can provide afterimage signals for later neurons. Our results indicate that afterimage signals are generated in the retina but may be modified like other retinal signals by cortical processes, so that evidence presented for cortical generation of color afterimages is explainable by spatiotemporal factors that modify all signals.

## Results

### Psychophysics

Color afterimages are common in everyday experience (and many popular web demonstrations). It has long been conjectured that afterimages result from neural adaptation, but adaptation is ubiquitous throughout the visual system, so the neural locus of afterimages has been elusive [7–9, 11–13]. We devised a simple psychophysical method of evoking afterimages and measuring the underlying adaptation (see [Movie S1](#) available online). A gray disk subtending 3.6° was divided into two halves. The colors of the two hemidisks were slowly modulated by sinusoidal half-cycles to opposite ends of a color axis, e.g., one half changed gray > violet > gray, whereas the other changed gray > lime green > gray in the complementary color direction ([Figure 1](#), top). The percepts of the hemidisks initially followed the stimulus but then accelerated past it, reaching gray before the stimulus and then continuing in the opposite directions to negative afterimages; e.g., when the physical modulations returned to gray, the half modulated through violet

appeared lime green and the half modulated through lime green appeared violet ([Figure 1](#), middle). By using a clock face at the fixation point ([Figure 1](#), bottom), with the clock's starting point perturbed randomly on each trial, we were able to have observers report the exact time that the two hemidisks appeared identical, which we call the “identity point.” At this point, despite the physical difference between the two sides, the neural signals must be equated by some stage of the visual system [10]. Hence, the physical contrast between the two hemidisks quantifies the modification of neural signals by visual adaptation, and we will call it the “nulled contrast.”

Evidence for afterimages resulting from adaptation in independent (L, M, S) cone classes [7] often used lights many orders of magnitude brighter than lights that generate afterimages in our method, thus causing pigment bleaching, but psychophysical evidence shows that afterimages of lights also occur at midphotopic levels [13]. In addition, retinal ganglion cells (RGCs) are the earliest neurons in the primate visual system to have been recorded from *in vivo*. Consequently, to search for an early neural substrate, we calibrated a display system to produce modulations around a midgray (62.85 cd/m<sup>2</sup>) along the three color axes that evoke maximal responses from RGCs [14]. Using the abbreviations KC, PC, and MC for cells projecting to konio-, parvo-, and magnocellular layers of lateral geniculate nucleus, respectively, these axes are  $\Delta(S)$  for KC cells,  $\Delta(L-M)$  for PC, and  $\Delta(L+M+S)$  for MC [15], i.e., the cardinal color axes [16, 17].

[Figure 2](#) shows the timing of the psychophysical identity points expressed as radians of the stimulus modulation (0 to  $\pi$ ), and the corresponding nulled contrasts as fractions of the stimulus contrast for the three cardinal axes. Each plotted point is the mean of 100 measurements spread randomly over 30 sessions. The mean identity points ranged from 0.85 $\pi$  to 0.98 $\pi$  and were all significantly different from  $\pi$ . The corresponding nulled contrasts ranged from 0.47 to 0.07 and were all significantly different from 0.0. All six observers showed less proportional adaptation for the  $\Delta(L+M+S)$  modulation than for the  $\Delta(L-M)$  modulation. The former stimulus provides almost ten times as much cone photoreceptor modulation as the latter, so the difference in relative adaptation could indicate that the relevant adaptation occurs after the combination of cone signals.

### Electrophysiology

To directly locate the neural substrate of color afterimages, we measured parafoveal neuronal responses for five KC, nine PC, and seven MC ganglion cells in anesthetized macaques, using well-established methods [18]. Each cell was exposed to sinusoidal modulation from gray to each pole of its preferred cardinal axis. The stimuli for KC and PC were 5° uniform circular patches covering the receptive fields. The stimuli for MC were stationary sinusoidal gratings of spatial frequency 0.5 cpd, with the cell centered at the peak or trough. Uniform fields generated weaker effects from MC cells. [Figures 3A–3C](#) show spike histograms of typical KC, PC, and MC responses, respectively. In each case, the responses of RGCs tracked modulation in their preferred direction but decreased to the prestimulus rate well before the physical modulation returned to gray, dipped below this level, and then recovered slowly. Cell responses to color modulation in the opposite direction showed the

\*Correspondence: qz@sunyopt.edu

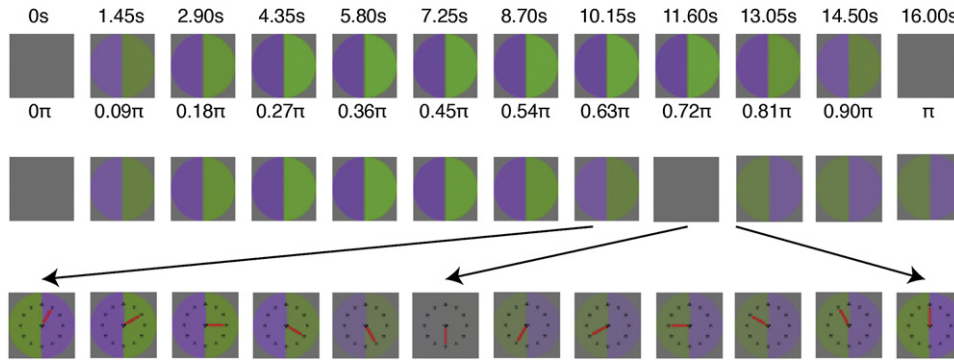


Figure 1. Psychophysical Procedure

Top shows half cycle of sinusoidal stimulus modulation (1/32 Hz presented at 120 frames/sec) depicted for this figure at 1.45 s and 0.09 radian intervals. Middle shows approximate percept corresponding to the stage of stimulus modulation immediately above. The two halves reach identity perceptually before they do physically. Bottom shows that the segment of trial around the point of identity is expanded to show how the clock face is used to make the measurement. A supplemental movie of the procedure is linked to the online version.

reverse pattern. Slow neural adaptation of the RGC population can account for the after images: cells responding at gray after the cessation of the modulation will propagate an afterimage signal to subsequent stages. Figure 4 provides data on all the cells we recorded. Figure 4A illustrates the robustness of rebound responses. The fitted line shows that on average, the rebound response of the cell expressed as change in number of spikes/sec from the baseline was 42% of the maximum response to the stimulus.

### Models of Cell Adaptation

For every instant  $t$ , the deviation of the response  $R(t)$  from the prestimulus firing-rate  $R(0)$  was well fit by an adaptive model that subtracts an accumulating, but exponentially decaying, postreceptor signal  $A(t)$  from the signal  $Q(t)$  generated by the current stimulus (Figure 5; Equation 1):

$$R(t) = R(0) + \omega Q(t) - \kappa A(t)^p \quad (1)$$

$$A(t) = (A(t - \Delta t) + \omega Q(t - \Delta t))e^{-\frac{\Delta t}{\tau}} \quad (2)$$

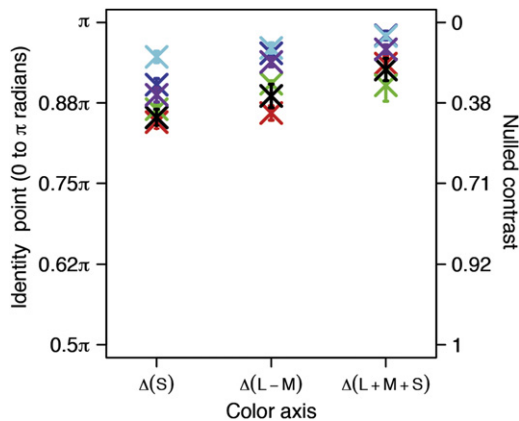


Figure 2. Identity Points for Afterimage Measurements

Averages of 100 trials for six observers are expressed as radians of the 1/32 Hz physical modulation and as nullified contrasts for the three cardinal color axes. Vertical bars indicate  $\pm 1$  SEM. Each observer is represented by the same color for the three axes.

Figures 3A–3C show the model's fits to the trajectories of the spike histograms, compared to the unadapted waveforms with the same trajectories as the stimuli. Figure 4B shows the distribution of zero crossings versus time constants for all cells. The estimated time constants of the exponential decay ranged from 4.8 to 17.6 s (almost all in the 5–12 s range), whereas at these light levels, evidence from primate horizontal cells suggests that cone adaptation is complete within a few msec, with time constants around 0.01 s [19]. We found that an exponent of 3 for  $A(t)$  provided much better fits than an exponent of 1, while preserving the sign of  $A(t)$ . Note that an exponent on the slow subtractive-adaptation signal will not affect the contrast-response curve, which is conventionally measured at higher temporal frequencies. The subtractive formulation feels intuitive and is similar to treatments of slow psychophysical adaptation [20–23], but it is difficult to conceive of accumulating and subtracting a feed-forward signal all within one cell. In compartmental models of neurons, shunting inhibition leads to subtractive adaptation [24, 25], but these models have not been tested for RGCs, where the inhibitory signal will need to have the same cone combination as the adapting cell. On the other hand, models consisting solely of multiplicative adaptation at the receptor and/or postreceptor stages are unable to account for the cell responses.

Figure 4B shows that cell responses cross the prestimulus response levels in the interval between  $0.68\pi$  to  $0.95\pi$ . The physiological zero crossings in Figure 4B cover the range of the psychophysical identity points in Figure 2, while being slightly earlier on average, and are thus consistent with our psychophysiological linking hypothesis and demonstrate that RGC adaptation is sufficient to account for the afterimages. A slight delay might be expected in registering the identity point due to locating the position of the clock hand. The psychophysical differences between different color directions are systematic but small, so given the variability in neural zero crossings, it would require a much larger sample of cells to test this difference reliably.

Consistent with the slow time constant, RGCs did not exhibit any significant adaptation to half a cycle of sine modulation at 2 Hz, and the perceptual afterimage for this stimulus was fleeting and barely visible. Because the estimated time constants were two to three orders of magnitude slower than photoreceptor adaptation, the adaptation must occur after the photoreceptors and at or before the RGCs.

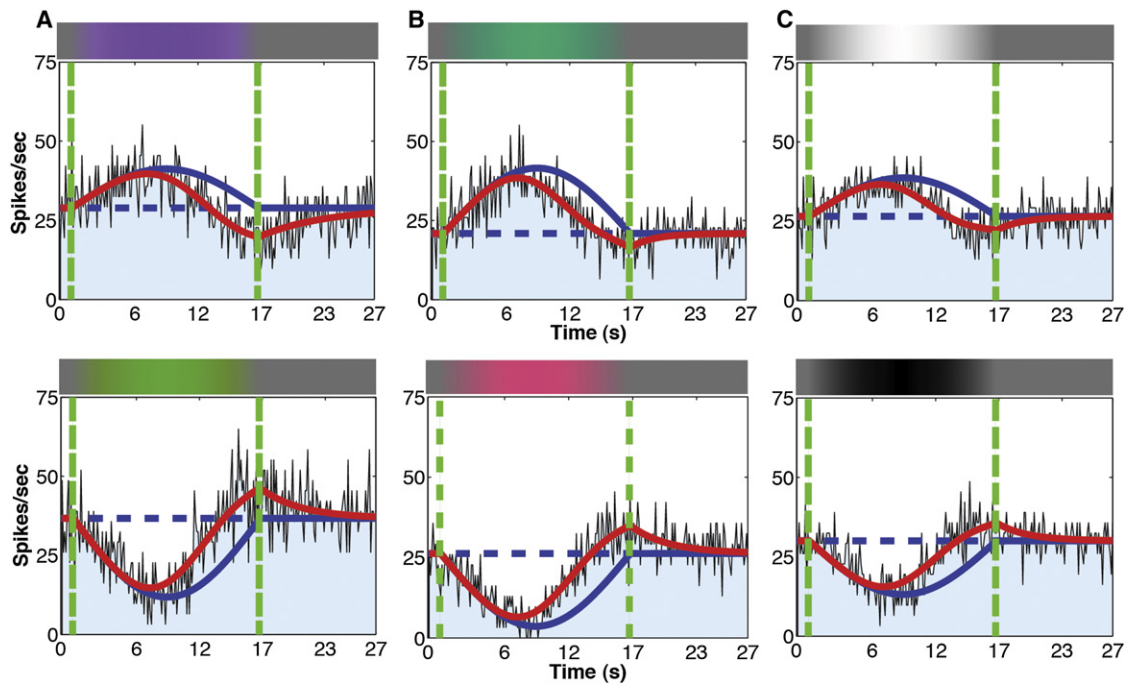


Figure 3. Ganglion Cell Responses to Slow Sinusoidal Modulations

(A) Histogram of +S-center KC spike responses to modulation toward violet (top) and yellow (bottom) pole of  $\Delta(S)$  axis. Solid red line represents best fit of adaptation model. Solid blue line represents response of cell without adaptation, which tracks the stimulus time course. Dashed blue line represents prestimulus response. Vertical green lines represent beginning and end of sinusoidal stimulus modulation.  
 (B) +M-center PC response to modulation toward green (top) and red (bottom) pole of  $\Delta(L-M)$  axis.  
 (C) ON-center MC response to modulation toward light (top) and dark (bottom) pole of  $\Delta(L+M+S)$  axis. Note that all responses return to prestimulus levels before the second green line and have the opposite polarity at that line.

### Discussion

This study shows that for lights considerably below photoreceptor bleaching levels, a postreceptor rebound response in retinal ganglion cells potentially constitutes an afterimage

signal. This result should correct the notion, found on the web and in many textbooks, that photoreceptor desensitization is responsible for color after-images generated by normal light levels. An elegant experiment has demonstrated afterimages generated by independent photoreceptors [7], but this

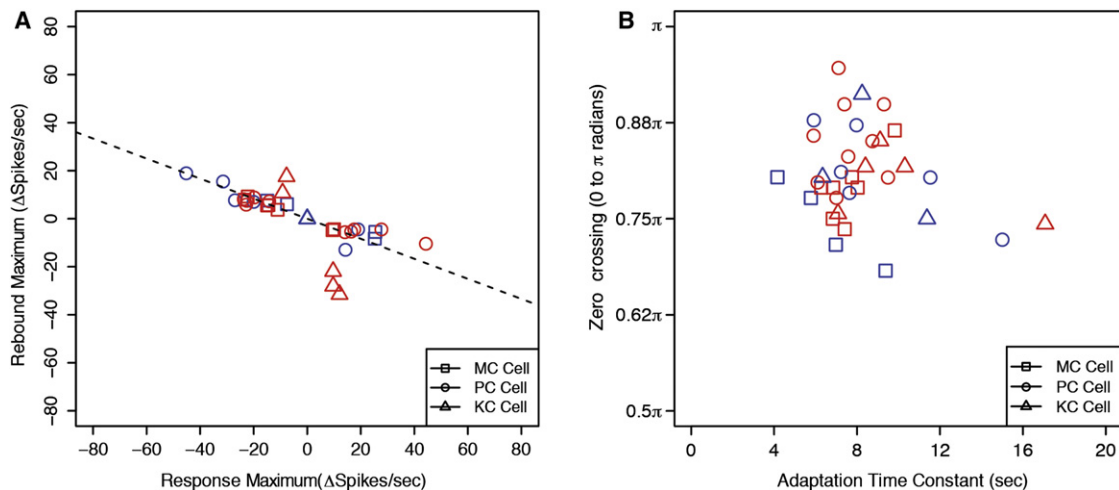


Figure 4. Summary of Neuronal Responses

(A) Maximum rebound response of each cell versus its maximum response to the stimulus (increments and decrements of spikes/sec). The best fitting regression line through (0,0) has a slope of  $-0.42$  ( $R^2 = 0.54$ ).  
 (B) The phase of zero crossing (0 to  $\pi$  radians) of each cell versus its time constant for subtractive adaptation (s). Different symbols denote different classes of RGCs. In both figures, there are two points per cell, one for each polarity of the stimulus modulation, except for a few cells for which we could only record one polarity reliably. Red symbols denote ON cells, and blue symbols denote OFF cells.

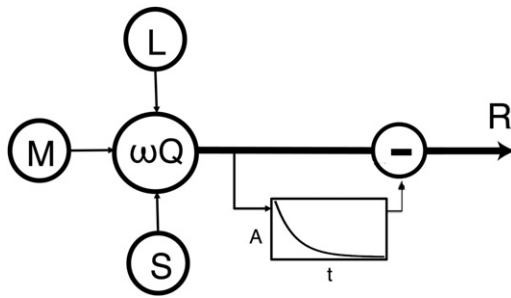


Figure 5. Schematic of Adaptation Model

L, M, S cone signals are combined at a postreceptor stage, and the accumulated signal of a leaky integrator is subtracted from the current signal (Equation 1).

requires intense lights that are bright enough to bleach substantial amounts of photopigment, so it is a photochemical, rather than neural, effect.

Because to thalamic and cortical cells, spikes transmitted as part of retinal rebound signals are no different from any other spikes from the retina, cortical processes, such as simultaneous contrast and selective attention, should be expected to modify afterimage signals. Thus, the visually striking demonstrations of these modifications [4, 6, 26, 27] may require no new mechanisms for their explanation. Similarly, retinal rebound signals should generate filling-in under the same spatial and temporal conditions as other retinal signals [5]. A claim for cortical generation of color afterimages has been based on stronger filling-in of afterimages from configurations that support an illusory filled-in surface interpretation than from those that do not [9]. Our sinusoidal modulation procedure revealed that the edges of the afterimages are much crisper in the “surface” conditions than in the “nonsurface” conditions of that study, and that the blurred edges reduce filling in, much like they do for physical stimuli. The other claim for cortical generation is based on binocularly misbound afterimages [8], but these only last for fractions of a second and may result from the habituation of cortical cells caused by repeated stimulus modulations or eye movements across edges [6, 16, 26, 28, 29]. Consequently, although cortical adaptation is responsible for many aftereffects, e.g., motion and tilt, our results make it unlikely that it generates color afterimages to prolonged viewing of moderate lights.

Our results utilized novel and simple psychophysical and electrophysiological procedures. The new psychophysical method is effective at evoking afterimages, makes possible a direct linking hypothesis between psychophysical and electrophysiological measurements [10], and is more precise than conventional afterimage duration measurements [6, 26]. The clock hand we used facilitates precise timing judgments without interfering with the primary percept, so it can be applied to many other experimental situations. Our electrophysiological method is a simple way to measure slow adaptation time constants of neurons [30] and does not rely on probes that could disturb adaptation state [31]. In addition, we have previously demonstrated that slow sinusoidal modulations of motion, tilt, size, etc. also generate the corresponding aftereffects, so our methods can be generalized to other aftereffects and their underlying adaptations in other neural areas.

## Experimental Procedures

The psychophysics experiments were conducted in compliance with the standards set by the Internal Review Board at the SUNY College of Optometry, and all physiology procedures strictly conformed to the National Institutes of Health Guide for the Care and Use of Laboratory Animals and were approved by the Animal Care and Use Committee.

## Supplemental Information

Supplemental Information includes one movie and can be found with this article online at doi:10.1016/j.cub.2011.12.021.

## Acknowledgments

We thank Jose-Manuel Alonso and Steve Shevell for their comments on an early draft. This work was partially funded by National Eye Institute grants EY07556, EY13312, EY13112, and EY019651.

Received: October 10, 2011

Revised: November 14, 2011

Accepted: December 6, 2011

Published online: January 19, 2012

## References

1. Sabra, A.I., ed. (1989). *The Optics of Ibn Al-Haytham. Books I-III. On Direct Vision* (London: The Warburg Institute).
2. Turnbull, H.W. (1961). *The Correspondence of Isaac Newton, Vol. 3, 1688–1694* (Cambridge: Cambridge University Press).
3. Wheatstone, C. (1838). Contributions to the physiology of vision-Part the first. On some remarkable, and hitherto unobserved, phenomena of binocular vision. *Philosophical Transactions of the Royal Society* 128, 371–394.
4. Tse, P.U., Kohler, P.J., and Reavis, E.A. (2010). Attention modulates perceptual rivalry within after-images. *J. Vis.* 10, 194.
5. van Lier, R., Vergeer, M., and Anstis, S. (2009). Filling-in afterimage colors between the lines. *Curr. Biol.* 19, R323–R324.
6. van Boxtel, J.J.A., Tsuchiya, N., and Koch, C. (2010). Opposing effects of attention and consciousness on afterimages. *Proc. Natl. Acad. Sci. USA* 107, 8883–8888.
7. Williams, D.R., and MacLeod, D.I.A. (1979). Interchangeable backgrounds for cone afterimages. *Vision Res.* 19, 867–877.
8. Shevell, S.K., St Clair, R., and Hong, S.W. (2008). Misbinding of color to form in afterimages. *Vis. Neurosci.* 25, 355–360.
9. Shimojo, S., Kamitani, Y., and Nishida, S. (2001). Afterimage of perceptually filled-in surface. *Science* 293, 1677–1680.
10. Brindley, G.S. (1970). *Physiology of the Retina and the Visual Pathway, Second Edition* (Baltimore: Williams & Wilkins).
11. Craik, K.J.W. (1940). Origin of Visual After-images. *Nature* 145, 512–512.
12. Kelly, D.H., and Martinez-Uriegas, E. (1993). Measurements of chromatic and achromatic afterimages. *J. Opt. Soc. Am. A* 10, 29–37.
13. Loomis, J.M. (1972). The photopigment bleaching hypothesis of complementary after-images: a psychophysical test. *Vision Res.* 12, 1587–1594.
14. Zaidi, Q., and Halevy, D. (1993). Visual mechanisms that signal the direction of color changes. *Vision Res.* 33, 1037–1051.
15. Sun, H., Smithson, H.E., Zaidi, Q., and Lee, B.B. (2006). Specificity of cone inputs to macaque retinal ganglion cells. *J. Neurophysiol.* 95, 837–849.
16. Krauskopf, J., Williams, D.R., and Heeley, D.W. (1982). Cardinal directions of color space. *Vision Res.* 22, 1123–1131.
17. Derrington, A.M., Krauskopf, J., and Lennie, P. (1984). Chromatic mechanisms in lateral geniculate nucleus of macaque. *J. Physiol.* 357, 241–265.
18. Lee, B.B., Martin, P.R., and Valberg, A. (1989). Sensitivity of macaque retinal ganglion cells to chromatic and luminance flicker. *J. Physiol.* 414, 223–243.
19. Smith, V.C., Pokorny, J., Lee, B.B., and Dacey, D.M. (2008). Sequential processing in vision: The interaction of sensitivity regulation and temporal dynamics. *Vision Res.* 48, 2649–2656.
20. Hayhoe, M.M., Benimoff, N.I., and Hood, D.C. (1987). The time-course of multiplicative and subtractive adaptation process. *Vision Res.* 27, 1981–1996.

21. Rinner, O., and Gegenfurtner, K.R. (2000). Time course of chromatic adaptation for color appearance and discrimination. *Vision Res.* **40**, 1813–1826.
22. Shapiro, A., Beere, J., and Zaidi, Q. (2001). Stages of temporal adaptation in the RG color system. *Color Res. Appl.* **26**, S43–S47.
23. Shapiro, A., Beere, J., and Zaidi, Q. (2003). Time course of adaptation stages in the S cone color system. *Vision Res.* **43**, 1135–1147.
24. Holt, G.R., and Koch, C. (1997). Shunting inhibition does not have a divisive effect on firing rates. *Neural Comput.* **9**, 1001–1013.
25. Silver, R.A. (2010). Neuronal arithmetic. *Nat. Rev. Neurosci.* **11**, 474–489.
26. Anstis, S.M. (1967). Visual adaptation to gradual change of intensity. *Science* **155**, 710–712.
27. Anstis, S., Rogers, B., and Henry, J. (1978). Interactions between simultaneous contrast and coloured afterimages. *Vision Res.* **18**, 899–911.
28. Zaidi, Q., Spehar, B., and DeBonet, J.S. (1998). Adaptation to textured chromatic fields. *J. Opt. Soc. Am. A Opt. Image Sci. Vis.* **15**, 23–32.
29. Tailby, C., Solomon, S.G., Dhruv, N.T., and Lennie, P. (2008). Habituation reveals fundamental chromatic mechanisms in striate cortex of macaque. *J. Neurosci.* **28**, 1131–1139.
30. Bonds, A.B. (1991). Temporal dynamics of contrast gain in single cells of the cat striate cortex. *Vis. Neurosci.* **6**, 239–255.
31. Yeh, T., Lee, B.B., and Kremers, J. (1996). The time course of adaptation in macaque retinal ganglion cells. *Vision Res.* **36**, 913–931.